



# Influence mechanisms of textile-dyeing sludge characteristics on degradation of anilines by integrated ultrasound-permanganate treatment



Jieying Liang, Xun-an Ning\*, Xiaojun Lai, Haiyuan Zou, Jian Sun, Xingwen Lu, Yaping Zhang, Taicheng An

School of Environmental Science and Engineering, Institute of Environmental Health and Pollution Control, Guangdong University of Technology, Guangzhou, 510006, China

## ARTICLE INFO

### Article history:

Received 17 October 2016  
Received in revised form  
15 December 2016  
Accepted 10 March 2017  
Available online 11 March 2017

### Keywords:

Cleaner production  
Anilines  
Textile-dyeing sludge  
Ultrasound-permanganate  
Sludge characteristics

## ABSTRACT

In order to support the use of integrated ultrasound-Mn(VII) for the removal of anilines, this study investigated for the first time the influence of the sludge characteristics on the reaction kinetics of target anilines including *o*-toluidine, *p*-chloroaniline, 2-methoxy-5-methylaniline, and 2,4,5-trimethylaniline. The results indicated that with a  $\text{KMnO}_4$  dosage of 1 mM and an ultrasound power density of  $0.90 \text{ W cm}^{-3}$ , 68.85%, 85.53%, and 78.50% of anilines can be removed from textile sludge plant 1, 2, and 3. Higher removal efficiency of anilines was achieved at a lower pH value, smaller particle size, and more negative  $\zeta$ -potential. The target anilines exhibited substantial reactivity toward Mn(VII) with the maxima of second-order rate constants at a pH value near their  $\text{pK}_a$  values for *o*-toluidine ( $0.80 \text{ M}^{-1}\text{s}^{-1}$  at pH 4), *p*-chloroaniline ( $0.65 \text{ M}^{-1}\text{s}^{-1}$  at pH 4), 2-methoxy-5-methylaniline ( $0.45 \text{ M}^{-1}\text{s}^{-1}$  at pH 4), and 2,4,5-trimethylaniline ( $0.34 \text{ M}^{-1}\text{s}^{-1}$  at pH 5). Moreover, the biodegradability of textile-dyeing sludge was greatly enhanced by integrated ultrasound-Mn(VII) treatment. This integrated treatment was proposed as an effective method for the disposal of anilines in textile-dyeing sludge.

© 2017 Elsevier Ltd. All rights reserved.

## 1. Introduction

Due to the toxic, carcinogenic and mutagenic of aromatic amines, 22 aromatic amines have been prohibited by Regulation (European Union) 1907/2006, and 24 have been banned in China (GB/T 17592-2011). However, the banned aromatic amines had been detected in the school uniforms in Shanghai, China in 2013. The banned aromatic amines were also detected in the textile-dyeing sludge by our previous study (Ning et al., 2015). The concentrations of *o*-toluidine (*o*-T), *p*-chloroaniline (PCA), 2-methoxy-5-methylaniline (MMA) and 2,4,5-trimethylaniline (TMA) in textile-dyeing sludge were determined as high as 6.11, 1.17, 3.075 and  $0.435 \mu\text{g g}^{-1}$  dry weight in textile-dyeing plants of Guangdong Province. The main source of *o*-T, PCA, MMA and TMA could be from azo dyes degradation through wastewater treatment process (van der Zee and Villaverde, 2005). Banned anilines

has raised serious concerns regarding their adverse effect on the environment (Ning et al., 2015).

Advance oxidation processes (AOPs) include in-situ chemical oxidation with ozone, Fenton reagents, ferrate, free chlorine, chlorine dioxide, sulfate radicals, and Mn(VII). Among them, Mn(VII) is usually the preferred one for its effectiveness over a wide pH range, convenient operation, comparative stability, mobility in the subsurface, and relatively low cost (Jiang et al., 2012; Sun et al., 2013). Ultrasound is also a useful method because of its desorption effect, free radical oxidation of supercritical water, mechanical shearing action, and increasing mass transfer effect. Effective removal of pollutants in aqueous systems or sludge has been proven in previous studies. Zhou et al. (2008) reported that in the combined ultrasound-Fe/EDTA system, the degradation rate constant of 2,4-dichlorophenol was 7 and 32 times higher than that in Fe/EDTA only and ultrasound only system, respectively. Lin et al. (2016) found that degradation of PAHs in textile-dyeing sludge when using combined ultrasound-Fenton (73.0%) was higher than the degradation by Fenton only (70.3%) and by ultrasound only (41.4%) in 60 min. According to our previous methods (Liang et al.,

\* Corresponding author.

E-mail addresses: [ningxunan666@126.com](mailto:ningxunan666@126.com), [2218414257@qq.com](mailto:2218414257@qq.com) (X.-a. Ning).

2016) employed for the degradation of aromatic amines in textile-dyeing sludge, ultrasound not only enhanced the entrance of Mn(VII) into the sludge to accelerate the reaction of Mn(VII) with the strongly adsorbed aromatic amines but also separated the pollutants from the sludge. Approximately 58.7% of monocyclic anilines and 88.3% of other forms of aromatic amines were removed by integrated ultrasound-Mn(VII) under the optimal operating conditions.

Many studies mainly focused on the removal of dyes (Lee et al., 2016; Chong et al., 2015). Only a few studies have been conducted on the degradation of banned anilines in the gas-phase by catalytic oxidation systems (An et al., 2010, 2011). Few researchers studied the consistency of the effect on textile-dyeing processes of different characteristics on the sludge. Textile-dyeing sludge is a very complex mixture, not only containing dyes, heavy metal ions, surfactants, solvents, and detergents but also some degradation products including polycyclic aromatic hydrocarbons (PAHs), aromatic amines, and other recalcitrant compounds (Ning et al., 2014a,b, 2015). Jonsson et al. (2009) has discovered that soil characteristics (e.g. pH, organic matter, particle size, and specific surface area) and PAH properties greatly influenced the degradation of PAHs in contaminated soils by Fenton's reagent. The humic substances in the background were also found to enhance the oxidation of phenols by Mn(VII) at acidic conditions (Sun et al., 2013). Thus, the characteristics of the sludge matrix may strongly influence the degradation of anilines in textile-dyeing sludge. To support the use of integrated ultrasound-Mn(VII) for the removal of anilines, a detailed understanding of the influence of the mechanisms of textile-dyeing sludge characteristics on reaction kinetics is desirable. Reliable values of second-order rate constants [ $k_{\text{Mn(VII)}}$ ] have been widely reported for the degradation of phenolic compounds (Jiang et al., 2012; Du et al., 2012), chlorinated organic compounds (Kao et al., 2008), antibiotics (Hu et al., 2009, 2010), and many other pollutants (Waldemer and Tratnyek, 2006). They are well known to be oxidised by Mn(VII), however, the available kinetic data on anilines degradation are not sufficient to determine the  $k_{\text{Mn(VII)}}$ 's activities. Therefore, investigation on the degradation kinetics of anilines in textile-dyeing sludge influenced by the characteristics of treatment with integrated ultrasound-Mn(VII) is of considerable importance.

The objective of this study was to investigate the influence of the mechanisms of textile-dyeing sludge characteristics (the content of organic matter, pH, particle size, and  $\zeta$ -potential) on the oxidation kinetics of target anilines (o-T, PCA, MMA and TMA) in concentrated sludge by integrated ultrasound-Mn(VII) treatment. The  $k_{\text{Mn(VII)}}$  for the reaction of integrated ultrasound-Mn(VII) with target anilines in the sludge was measured over a pH range of 4–9. Biodegradability was examined for the extracted solution from three types of textile-dyeing sludge for further verification of the effect of ultrasound-Mn(VII) treatment.

## 2. Experimental section

### 2.1. Materials

Target anilines including o-T, PCA, MMA, and TMA, each at the concentration of 100 mg L<sup>-1</sup> were used in this study. Naphthalene-d8 and aniline-d5 at the concentration of 2000 mg L<sup>-1</sup> were used as internal standard and surrogate standard, respectively. Analytical conditions and a chromatogram of target anilines in the standard solution are shown in Table S1 and Fig. S1. All chemical standards were obtained from O2si Smart Solutions (Charleston, SC, USA) with a purity > 99.5%. High-performance liquid chromatography (HPLC)-grade methanol and methyl tert-butyl ether were purchased from Fisher Scientific (USA). Deionized water (18.25 M $\Omega$  cm) was

obtained by passing distilled water through a Millipore Milli-Q water purification system. Other chemicals were of analytical grade or better and used without further purification. Stock solutions of Mn(VII) were prepared by dissolving the crystals of KMnO<sub>4</sub> in deionized water and standardized spectrophotometrically by UV detection at 525 nm ( $\epsilon = 2500 \text{ M}^{-1}\text{cm}^{-1}$ ). Most of anilines were generated through sequential anaerobic-aerobic reactor systems in wastewater treatment. Following, the generated anilines were concentrated in a concentrated tank. Moreover, concentrated tank reduces the moisture content of the sludge but still remained liquidity, thus, concentrated sludge from the textile-dyeing plant was chosen to investigate the potential of integrated ultrasound-Mn(VII) as a polishing step for enhancing the removal of anilines. Raw sludge samples were collected from the concentrated tanks of three representative textile-dyeing plants (TDP1, TDP2, and TDP3) in Dongguan, Guangdong Province, China, in March, 2016. The sludges were stored in a freezer at 4 °C and the experimental sludge samples were used within a week. The main characteristics of the raw sludges and the details of main processes, material, dyes applied in the textile-dyeing plants are listed in Table 1.

### 2.2. Experiments and analysis

The experimental set-up is briefly described in Text S1 in Supporting Information (SI). Each reaction was initiated by quickly adding Mn(VII) while the mixture was being sonicated. Samples were periodically collected and quenched with hydroxylamine. The slurry of samples was centrifuged at 4000 rpm for 10 min. The sludge matrix was freeze-dried using an LGJ-12 vacuum freeze dryer (Songyuan Huaxing Technology Development Co., Ltd., Beijing, China) and stored in a refrigerator at -4 °C until analysis.

The extraction method and GC-MS analytical method are described in Text S2 in SI. Mn(VII) concentrations at low micromolar range were simultaneously determined in a second sample by the ABTS spectrophotometric method (see Text S3 in SI for the details). Mn(VII) concentrations at high micromolar range were measured by UV detection at 525 nm ( $\epsilon = 2500 \text{ M}^{-1}\text{cm}^{-1}$ ) prior to being quenched with hydroxylamine during the kinetic runs. Samples were filtered prior to analysis to eliminate the interference from MnO<sub>2</sub> precipitate. The sludge medium particle size ( $d_{50}$ ) before and after the integrated ultrasound-Mn(VII) treatment was examined using a laser particle size analyser (Eye Tech, Ankersmid, Netherlands). The  $\zeta$ -potential measurements of the sludge before and after the integrated US-Mn(VII) treatment were obtained using a Malvern ZetaSizer 2000 (Malvern, UK) which measures the electrophoretic mobility and converts this to  $\zeta$ -potential based on the Smoluchowski Approximation when  $\kappa_a \gg 1$ . To determine the loss-on-ignition, which is a measure of the organic matter content in textile-dyeing sludge, about 10 g wet sludge matrix samples were dried overnight at 105 °C, weighed, then baked in an oven for 2 h at 550 °C and reweighed. The values of chemical oxygen demand (COD<sub>Cr</sub>) and biochemical oxygen demand (BOD<sub>5</sub>) were measured according to standard methods 5220C and 5210B (APHA, 1998). The dichromate method was used for COD<sub>Cr</sub> measurement. The five-day cultivation method (20 ± 1 °C) was used to determine the concentration of BOD<sub>5</sub>. The content of Mn was determined by atomic absorption spectrometry (AAS, Z-2000, Hitachi). The statistical package, SSPS 19, was used for variance analysis.

Degradation kinetic reactions were initiated by adding excess Mn(VII) of 0.1–4 mM into the pH-buffered textile-dyeing sludge under a fixed ultrasound power density of 0.9 W cm<sup>-3</sup>. The oxidation kinetics of target anilines (o-T, PCA, MMA, and TMA) by integrated ultrasound-Mn(VII) in TDP1 were examined following the same procedure as that in the raw textile-dyeing sludge. Sodium acetate was used for adjusting textile-dyeing sludge at pH

**Table 1**  
Characteristics of the raw textile-dyeing sludges.

Parameters	TDP 1	TDP 2	TDP 3
Main treatment processes	A/O, flocculation	Flocculation, A/O	A, flocculation, O
Material	Chemical fiber	Mix	Cotton
Dyes	Ion dyes, acid dyes	Mix	Ion dyes, disperse dyes
Sludge organic matter content (%)	49.82 ± 0.41	66.61 ± 0.27	51.78 ± 0.86
Moisture content (%)	98.58 ± 0.01	99.16 ± 0.01	98.12 ± 0.01
pH <sub>(H2O)</sub>	7.75 ± 0.01	6.67 ± 0.00	6.91 ± 0.00
COD <sub>Cr</sub> (mg/L)	84266 ± 84	96533 ± 93	65450 ± 156
BOD <sub>5</sub> (mg/L)	8425 ± 20	8396 ± 17	5742 ± 50
o-T (μg kg <sup>-1</sup> dw sludge)	865.02 ± 25.36	348.43 ± 31.27	187.50 ± 20.10
PCA (μg kg <sup>-1</sup> dw sludge)	483.68 ± 20.12	418.55 ± 18.56	487.70 ± 23.34
MMA (μg kg <sup>-1</sup> dw sludge)	239.33 ± 27.35	866.46 ± 19.23	949.59 ± 32.23
TMA (μg kg <sup>-1</sup> dw sludge)	358.22 ± 12.32	370.93 ± 16.56	565.99 ± 21.21
Recoveries of the anilines in sludge (%)		55–96	
Recoveries of aniline-d5 (%)		73–87	

TDP: Textile-dyeing Plant.

A: Anaerobic; O: Aerobic.

4–6. The pH values of textile-dyeing sludge were maintained at an approximately constant level ( $\pm 0.1$ ) by the addition of HCl or NaOH if necessary. All the kinetic experiments were conducted at  $25 \pm 1$  °C in duplicate or triplicate.

### 3. Results and discussion

#### 3.1. Degradation of anilines in three textile-dyeing sludges by integrated ultrasound-Mn(VII) treatment

The removal of anilines by integrated ultrasound-Mn(VII) was investigated in three textile-dyeing sludges, the properties of which are summarized in Table 1. Fig. 1 shows the removal efficiencies of anilines in three textile-dyeing sludges with 1 mM Mn(VII) and an ultrasound power density of  $0.90 \text{ W cm}^{-3}$ . The results showed a general trend of enhanced anilines removal with time. In the first 5 min, the average removal rates of four anilines in three textile-dyeing sludges (TDP1, TDP2, and TDP3) were 44.81%, 37.75%, and 39.23%, respectively. At 30 min, anilines decreased gradually and reached an average maximum removal efficiency of 68.85%, 85.53%, and 78.50%. The maximum removal efficiencies of o-T, PCA, MMA, and TMA were 87.56%, 80.19%, 92.84%, and 79.63% in TDP2, respectively, whereas only 49.12% of o-T and 70.38% of TMA were removed in TDP3, and 64.00% of PCA and 56.00% of MMA were removed in TDP1. The variation in the removal efficiencies of anilines among three textile-dyeing sludges may be ascribed to the differences in key sludge quality characteristics, including sludge organic matter content, pH, particle size, and  $\zeta$ -potential (Tables 1 and 2). Further explanation is provided in Section 3.2.1.

#### 3.2. The influence of the characteristics of textile-dyeing sludge on the degradation of anilines by integrated ultrasound-Mn(VII) treatment

##### 3.2.1. Organic matter

As seen in Fig. 2, the initial organic matter contents of three textile-dyeing sludges (TDP1, TDP2, and TDP3) were 49.82%, 51.78%, and 66.61%, respectively. In the first 5 min, the organic matter contents of sludge decreased to 48.17%, 49.71%, and 58.71%, and then continued to decrease steadily. Organic matter reacts with Mn(VII) because Mn(VII) has a strong ability to oxidize organic matter that contains electron-rich sites. Further, organic matter may be transferred to the supernatant after the ultrasound treatment since ultrasound presents obvious advantages for sludge floc structure disintegration (Ning et al., 2014a,b). The organic matter contents of TDP1, TDP2, and TDP3 at 30 min were 46.64%, 46.28%, and 46.35%. Both the organic matter and anilines contents of textile-dyeing sludges decreased with the reaction time. As shown in Fig. 2, the organic matter content of TDP3 was higher than TDP2 and the removal of target anilines in TDP3 was less than that in TDP2. This result suggests the organic matter may inhibit the degradation efficiency of anilines in textile-dyeing sludge due to the simultaneous reaction of Mn(VII) with electron-rich sites in organic matter. Jonsson et al. (2009) found that organic matter was one of the strongest competing factors for the degradation of the PAHs; the degradation of PAHs decreased if the organic matter content increased because they would compete with each other for the oxidant (e.g. OH). In many cases, the oxidant was simply consumed by organic matter prior to having a chance to react with

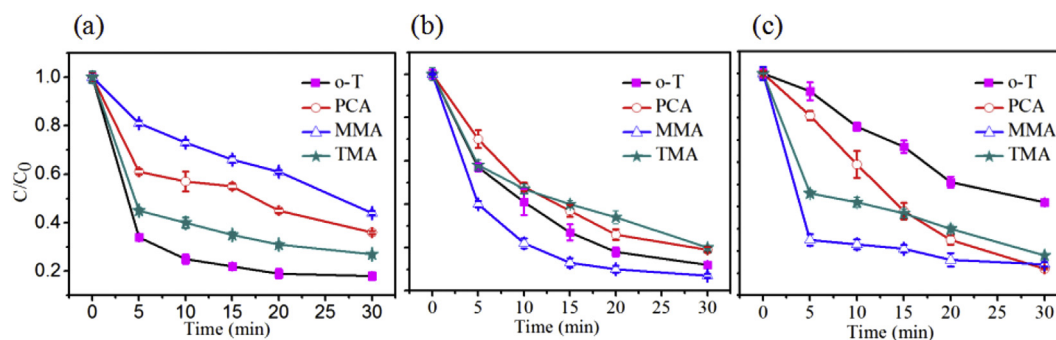


**Fig. 1.** The degradation kinetics of anilines in three textile-dyeing sludges (a) TDP1, (b) TDP2, and (c) TDP3 with a Mn(VII) dosage of 1 mM and an ultrasound power density of  $0.90 \text{ W cm}^{-3}$ .

**Table 2**  
Effects of integrated ultrasound-Mn(VII) on particle size and  $\zeta$ -potential.

Sludge samples	$d_{50}$ ( $\mu\text{m}$ )		$\zeta$ -potential (mV)	
	Raw sludge	Treated sludge	Raw sludge	Treated sludge
TDP 1	$35.30 \pm 0.05$	$10.85 \pm 0.02$	$-14.10 \pm 0.01$	$-18.68 \pm 0.01$
TDP 2	$19.86 \pm 0.08$	$7.18 \pm 0.11$	$-18.41 \pm 0.02$	$-22.26 \pm 0.02$
TDP 3	$23.15 \pm 0.12$	$7.36 \pm 0.09$	$-16.22 \pm 0.02$	$-21.73 \pm 0.02$

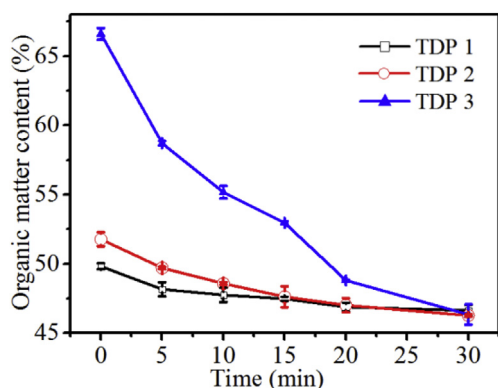


**Fig. 2.** The change of organic matter content in three textile-dyeing sludges with a Mn(VII) dosage of 1 mM and an ultrasound power density of  $0.90 \text{ W cm}^{-3}$ .

the target pollutants. Lindsey and Tarr (2000) confirmed that organic matter greatly influenced the degradation of pollutants; even low concentrations of dissolved natural organic matter could largely inhibit the degradation of hydrophobic compounds. In this study, organic matter in textile-dyeing sludge also reduced the effectiveness of Mn(VII) to react with target anilines by competing with Mn(VII).

However, the opposite result was obtained for TDP1 and TDP2. The organic matter content in TDP2 was higher than TDP1 and the anilines removal rate in TDP2 was also greater than in TDP1. The reductive sites in organic matter were found to be crucial for the oxidation of pollutants (e.g. phenols), because they could facilitate the in-situ formation of  $\text{MnO}_2$  which played a significant role in Mn(VII) reduction and worked as an oxidant (Sun et al., 2013) or catalyst (Jiang et al., 2014). Therefore, the role of organic matter in different TDPs in the degradation of anilines is not clear and warrants further research.

### 3.2.2. pH

In the raw textile-dyeing sludges, the pH had an influence on the degradation of anilines. The higher the pH (TDP1 > TDP3 > TDP2) was, the smaller the removal rate of anilines (TDP1 < TDP3 < TDP2) was (Table 1 and Fig. 1). No significant changes in the pH values were observed at the end of each reaction. In general, pH is one of the most important parameters for the oxidation potential of AOPs. To further confirm the influence of pH, TDP1 was chosen to investigate the reaction kinetics of anilines over the pH range of 4–9 by the integrated ultrasound-Mn(VII) treatment.

The reaction kinetics investigated here considered the Mn(VII) concentration at a fixed ultrasound power density of  $0.9 \text{ W cm}^{-3}$ . The kinetics of target anilines in batch reactions followed a pseudo-first-order rate law when the Mn(VII) concentration was much greater than the initial anilines concentration. As shown in Fig. S2a, the disappearance of anilines followed the pseudo-first-order kinetics with reaction time of 5–30 min at a Mn(VII) dosage of 4 mM and pH of 7. However, the disappearance of anilines did not follow the pseudo-first-order kinetics at 0–30 min, because it probably

needs time to balance the sludge system at 0–5 min. The rate constants ( $k_{\text{obs}}$ ) determined at various concentrations of Mn(VII) at pH 7 showed linearity with Mn(VII) concentrations at 5–30 min (Fig. S2b), indicating that the reaction was also a first-order reaction with respect to Mn(VII). Thus, the reaction kinetics for target anilines at 5–30 min followed a generalized second-order rate law (1):

$$\frac{d[\text{anilines}]}{dt} = K_{\text{obs}}[\text{anilines}] = k_{\text{Mn(VII)}}[\text{Mn(VII)}][\text{anilines}] \quad (1)$$

where  $k_{\text{obs}}$  was the pseudo-first-order rate constant for the reaction of Mn(VII) with each aniline at 5–30 min as a function of pH. The  $k_{\text{Mn(VII)}}$  was the second order rate constant, which was calculated by dividing  $k_{\text{obs}}$  by the concentration of Mn(VII).

The  $k_{\text{Mn(VII)}}$  values are shown in Fig. 3 and also illustrated in Table S2. As shown in Fig. 3, the  $k_{\text{Mn(VII)}}$  values for the target anilines increased with the decreasing pH, and the maxima occurred at pH values close to their  $\text{pK}_a$  values (e.g.  $\text{pK}_a$  values of o-T, PCA, and TMA were 4.44, 3.98 and 5.09). The maximum  $k_{\text{Mn(VII)}}$  values for the reaction were  $0.80 \text{ M}^{-1} \text{ s}^{-1}$  at pH 4 (o-T),  $0.65 \text{ M}^{-1} \text{ s}^{-1}$  at pH 4 (PCA),  $0.45 \text{ M}^{-1} \text{ s}^{-1}$  at pH 4 (MMA), and  $0.66 \text{ M}^{-1} \text{ s}^{-1}$  at pH 5 (TMA). Two degradation pathways between Mn(VII) and phenol were proposed by Du et al. (2012). On one of the pathways, the undissociated phenol would be directly oxidised by Mn(VII) to generate final products. On the other pathway, the dissociated phenol and Mn(VII) would form a phenol-Mn(VII) adduct, would be combined with  $\text{H}^+$ , and then decomposed to final products. Thus, for the same reason, Mn(VII) may have easily reacted with anilines when anilines' ions and molecules achieved balance. Similar results were also observed in previous studies. For instance, the  $k_{\text{Mn(VII)}}$  values for triclosan and 2,4-dichlorophenol achieved a maximum when pH approached to their  $\text{pK}_a$  values ( $\approx 8$ ), below or above which they decreased to lower magnitudes (Jiang et al., 2012). Waldemer and Tratnyek (2006) reported  $k_{\text{Mn(VII)}}$  values ranging from  $7 \times 10^{-6}$  to  $2 \times 10^2 \text{ M}^{-1} \text{ s}^{-1}$  for a wide range of organic compounds including chlorinated aromatic hydrocarbons, alkenes and alkanes, substituted phenols, and so on. In comparison with these ranges,

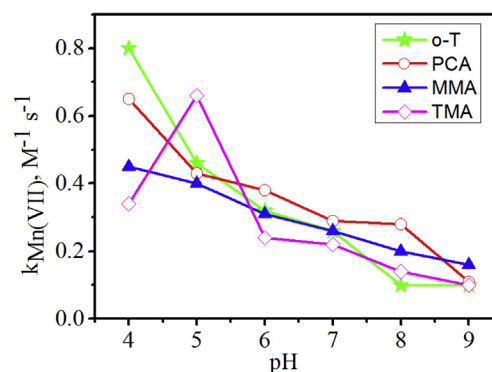


**Fig. 3.** Second-order rate constants ( $k_{\text{Mn(VII)}}$ ) for the reactions of integrated ultrasound-Mn(VII) with selected anilines at pH range of 4–9 within 5–30 min at  $25 \pm 1 \text{ }^\circ\text{C}$ .

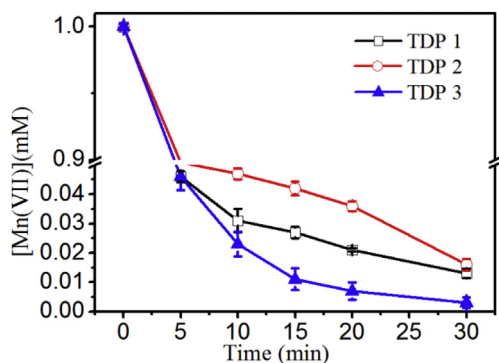


Fig. 4. The consumption kinetics of Mn(VII) in supernatant with a  $\text{KMnO}_4$  dosage of 1 mM and an ultrasound power density of  $0.90 \text{ W cm}^{-3}$ .

the four target anilines were within the more reactive middle of spectrum, which was much less reactive than the compounds that possessed highly Mn(VII)-reactive olefin and phenolic functional groups. The  $k_{\text{Mn(VII)}}$  value for the four target anilines is in the order of  $o\text{-T} > \text{TMA} > \text{PCA} > \text{MMA}$  at a pH near to their  $\text{pK}_a$ . The difference in values is caused by the fact that  $-\text{CH}_3$  in  $o\text{-T}$  and TMA is the electron-donating group, whereas  $-\text{Cl}$  in PCA is the electron-withdrawing group. Mn(VII) tends to react with the pollutants with more electron-donating groups. Jonsson et al. (2009) also found that physicochemical properties of PAHs affected their adsorption ability in soil, which is related to their degradation efficiencies in soil.

### 3.2.3. Particle size

The  $d_{50}$  values were analysed to investigate the effects of particle size on the degradation of anilines in the textile-dyeing sludge using the integrated ultrasound-Mn(VII) treatment (Table 2). The results showed that the smaller the particle size ( $\text{TDP2} < \text{TDP3} < \text{TDP1}$ ) was, the higher the removal efficiency of anilines ( $\text{TDP2} > \text{TDP3} > \text{TDP1}$ ) was. Sludge particles observed after the integrated ultrasound-Mn(VII) treatment were smaller than those in the untreated samples. The  $d_{50}$  were 35.30, 19.86, and 23.15  $\mu\text{m}$  in three raw textile-dyeing sludges, and decreased to 10.85, 7.18, and 7.36  $\mu\text{m}$  after treatment. The significant reduction of particle size achieved by the integrated ultrasound-Mn(VII) treatment may be attributed to the cavitation in the ultrasound condition, which created microturbulence and shock waves. The localized effect produced by microturbulence limitedly affected the particle size of sludge flocs and the drift generated by shock waves exerted a great force, therefore, large particles could be disrupted

increasing the number of smaller particles (Ning et al., 2014a,b). The smaller particle sizes increased the sludge surface area so that the Mn(VII) could efficiently react with anilines, which were strongly entrapped within the sludge cavities and tended to be less susceptible to Mn(VII) oxidation.

### 3.2.4. $\zeta$ -potential

The  $\zeta$ -potential is one of the most important characteristics of the sludge. Colloidal interactions between sludge particles are determined by various repulsive and attractive interparticle forces, which can be changed by the surface adsorption of organic polyelectrolytes and metal cations existing in the sludge. The  $\zeta$ -potential obtained in the raw and treated sludges are presented in Table 2. The more negative the  $\zeta$ -potential ( $\text{TDP2} < \text{TDP3} < \text{TDP1}$ ) was, the higher removal efficiency of anilines ( $\text{TDP2} > \text{TDP3} > \text{TDP1}$ ) was. The  $\zeta$ -potential values of  $-14.10$ ,  $-18.14$ , and  $-16.22$  mV were reported for three raw textile-dyeing sludges. After the treatment with integrated ultrasound-Mn(VII), the  $\zeta$ -potential (negative) had a tendency to decrease and finally reached  $-18.68$ ,  $-22.26$  and  $-21.73$  mV due to the change in metal cations and organic polyelectrolytes on the sludge surface. The more negative the  $\zeta$ -potential is, the greater the repulsion between particle is, resulting in a higher sludge-shear sensitivity and forming a larger number of sludge flocs per unit volume of sludge (Vogelaar et al., 2005). Anilines were contained on the surface and in the sludge, therefore at more negative  $\zeta$ -potentials, anilines tended to react with Mn(VII) to a greater extent.

The four single factors (organic matter, pH, particle size, and  $\zeta$ -potential) were analysed to eliminate the interference between each factor. The variance analysis was also conducted (Table S3). The p value of organic matter was 0.048, which was less than 0.05, indicating that organic matter had a significant influence on the removal of anilines. The p value of pH was 0.004, which was less than 0.01, indicating that pH had a very significant influence on the removal of anilines. However, the p value of the particle size was 0.507 and of  $\zeta$ -potential was 0.780, which were higher than 0.05, indicating that particle size and  $\zeta$ -potential had no significant influence on the removal of anilines. Thus, the order of the influence on the removal of anilines was  $\text{pH} > \text{organic matter} > \text{particle size} > \zeta\text{-potential}$ .

### 3.3. Mn release in supernate and in sludge

Fig. 4 shows the decay of Mn(VII) in the supernate of the textile-dyeing sludges at a Mn(VII) dose of 1 mM and an ultrasound power density of  $0.90 \text{ W cm}^{-3}$ . Mn(VII) decreased considerably in the first 5 min in the supernate. Cesaroa et al. (2014) indicated that the

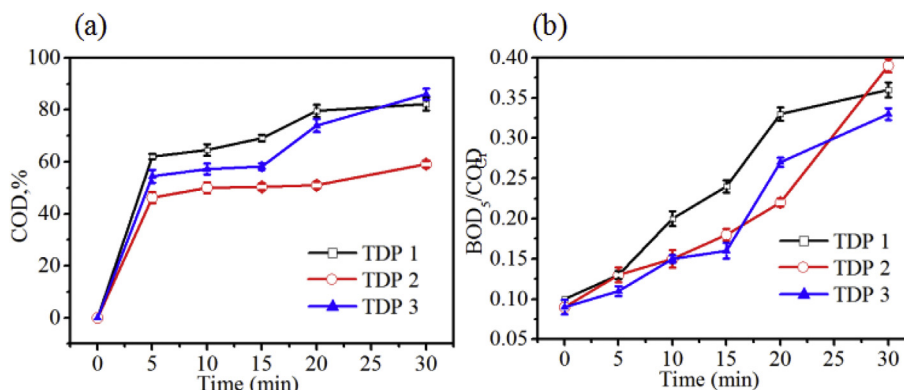


Fig. 5. COD removal efficiencies (a) and  $\text{BOD}_5/\text{COD}_{\text{Cr}}$  ratio (b) in three textile-dyeing sludges with a Mn(VII) dosage of 1 mM and an ultrasound power density of  $0.90 \text{ W cm}^{-3}$ .

cavitation phenomena produced by ultrasound could promote the solubilisation of organic matter, therefore, Mn(VII) could easily react with dissolved organic matter. The result was consistent with the degradation of anilines and organic matter in the textile-dyeing sludge. However, there was still a small amount of Mn(VII) in the supernate due to the intense agitation under the ultrasound condition (Fig. 4), because ultrasound could enhance the mass transfer of Mn(VII) in the supernate by increasing the volumetric mass transfer coefficient (Kuppa and Moholkar, 2010; Chakma and Moholkar, 2011). With the increase in reaction time, Mn(VII) concentration experienced a slight decrease and therefore Mn(VII) could simultaneously react with the organic matter when the organic matter was transferred to the supernate. Some Mn(VII) also entered the sludge again under the ultrasound condition. The content of Mn in the raw textile-dyeing sludge were 16.8, 961.5, and 291 mg kg<sup>-1</sup> in TDP1, TDP2, and TDP3, respectively. After the treatment with ultrasound-Mn(VII), the Mn content increased to 657.6, 2196.9, and 1995.4 mg kg<sup>-1</sup> dry weight, which is a little higher than that in municipal and industrial wastewater treatment plants (161–1844 mg kg<sup>-1</sup> dry weight) (Liu et al., 2015).

Note that in this study, Mn(VII) (1 mM) was used at a greater dosage than typically used in wastewater treatment facilities. Jiang et al. (2012) observed that the removal of endocrine disrupting chemicals was higher than 90% at the KMnO<sub>4</sub> dose of 0.012 mM. Pang et al. (2014) reported that the degradation of tetrabromobisphenol was over 80% in the treatment of real waters at the KMnO<sub>4</sub> dose of 0.006 mM. However, a smaller rate of removal of anilines (68–85%) would be expected in this study. The oxidation of organic compounds by integrated ultrasound-Mn(VII) produces MnO<sub>2</sub>, CO<sub>2</sub>, and organic intermediates. The presence of Mn(VII) and MnO<sub>2</sub> in textile-dyeing sludges may not usually constitute an environmental problem. However, excess MnO<sub>2</sub> precipitation can cause pore clogging, reduced permeability, and increased resistance to mass transfer after the textile-dyeing sludge was discarded on soil or in a landfill, which is an undesirable side effect and may affect the sludge quality. Thus, the appropriate Mn(VII) dosage depending on the specific sludge type should be added when using the integrated ultrasound-Mn(VII) method.

### 3.4. Biodegradability of three textile-dyeing sludges

The ratio of BOD<sub>5</sub> to COD<sub>Cr</sub> is generally regarded as the biodegradability index. In general, if the BOD<sub>5</sub>/COD<sub>Cr</sub> value is less than 0.30, the sludge is hardly biodegradable; if BOD<sub>5</sub>/COD<sub>Cr</sub> is between 0.30 and 0.45, the sludge is biodegradable; and if BOD<sub>5</sub>/COD<sub>Cr</sub> exceeds 0.45, the sludge is easily biodegradable (Sarría et al., 2002). As seen in Table 1, the COD<sub>Cr</sub> values in the initial raw sludges of TDP1, TDP2, and TDP3 were 84,266, 96,533, and 65,450 mg L<sup>-1</sup>, and BOD<sub>5</sub> concentrations were 8,425, 8,396, and 5742 mg L<sup>-1</sup>, corresponding to the BOD<sub>5</sub>/COD ratios of 0.10, 0.09, and 0.09, respectively. This means that the raw textile-dyeing sludge samples were hardly biodegradable prior to being treated by the integrated ultrasound-Mn(VII) treatment.

Overall, COD<sub>Cr</sub> in three textile-dyeing sludges under integrated ultrasound-Mn(VII) treatment was greatly removed in the first 5 min, and then gradually removed at the rates from 62.03 to 82.2%, 46.25 to 59.12%, 54.45 to 86.03%, respectively (Fig. 5), which is not surprising since Mn(VII) has a strong oxidation capability over a wider range of species containing electron-rich groups (Waldemer and Tratnyek, 2006). After the treatment, BOD<sub>5</sub>/COD<sub>Cr</sub> in three textile-dyeing sludges increased from 0.10 to 0.36, 0.09 to 0.39, 0.09 to 0.33, because of the decrease in COD<sub>Cr</sub>, whereas there was no obvious change in BOD<sub>5</sub> (the result is not shown). In other words, the biodegradability of the textile-dyeing sludges was largely enhanced by the integrated ultrasound-Mn(VII) treatment.

## 4. Conclusion

The integrated ultrasound-Mn(VII) treatment was found to be effective in degrading anilines in three types of textile-dyeing sludges. The order of the influence of textile-dyeing sludge characteristics on the removal of anilines was pH > organic matter > particle size > ζ-potential. Higher removal rates of anilines were achieved at lower pH, smaller particle size, and more negative ζ-potential. The target anilines exhibited substantial reactivity toward Mn(VII) with the maximum value of k<sub>Mn(VII)</sub> at pH values close to their pK<sub>a</sub> values because Mn(VII) easily reacted with anilines when anilines' ions and molecules achieved a balance. In addition, the biodegradability of textile-dyeing sludges was greatly increased by the integrated ultrasound-Mn(VII) treatment due to the strong oxidative power of Mn(VII) on a wide range of pollutants.

## Acknowledgments

This research was supported by the Natural Science Foundation of China (No. 21577027), the Science and Technology Plan of Guangzhou (201607010330), the Science and Technology Plan of Guangdong Province (No. 2015A020215032), and the Special Applied Technology Research and Development of Guangdong Province (major project) (No. 2015B020235013).

## Appendix A. Supplementary data

Supplementary data related to this article can be found at <http://dx.doi.org/10.1016/j.jclepro.2017.03.070>.

## References

- An, T.C., Sun, L., Li, G.Y., Wan, S.G., 2010. Gas-phase photocatalytic degradation and detoxification of o-toluidine: degradation mechanism and salmonella mutagenicity assessment of mixed gaseous intermediates. *J. Mol. Catal. A-Chemical* 333, 128–135.
- An, T.C., Sun, L., Li, G.Y., Gao, Y.P., Ying, G.G., 2011. Photocatalytic degradation and detoxification of o-chloroaniline in the gas phase: mechanistic consideration and mutagenicity assessment of its decomposed gaseous intermediate mixture. *Appl. Catal. B-Environ.* 102, 140–146.
- APHA, 1998. *The Standard Methods for the Examination of Water and Wastewater*, 20th-ed. American Public Health Association, Washington, DC.
- Cesaroa, A., Veltenb, S., Belgiorno, V., Kuchta, K., 2014. Enhanced anaerobic digestion by ultrasonic pretreatment of organic residues for energy production. *J. Clean. Prod.* 74, 119–124.
- Chakma, S., Moholkar, V.S., 2011. Mechanistic features of ultrasonic desorption of aromatic pollutants. *Chem. Eng. J.* 175, 356–367.
- Chong, M.N., Cho, Y.J., Poh, P.E., Jin, B., 2015. Evaluation of Titanium dioxide photocatalytic technology for the treatment of reactive Black 5 dye in synthetic and real greywater effluents. *J. Clean. Prod.* 89, 196–202.
- Du, J.S., Sun, B., Zhang, J., Guan, X.H., 2012. Parabola-like shaped pH-rate profile for phenols oxidation by aqueous permanganate. *Environ. Sci. Technol.* 46, 8860–8867.
- Hu, L., Martin, H.M., Arce-Bulted, O., Sugihara, M.N., Keating, K.A., Strathmann, T.J., 2009. Oxidation of carbamazepine by Mn(VII) and Fe(VI): reaction kinetics and mechanism. *Environ. Sci. Technol.* 43, 509–515.
- Hu, L.H., Martin, H.M., Strathmann, T.J., 2010. Oxidation kinetics of antibiotics during water treatment with potassium permanganate. *Environ. Sci. Technol.* 44, 6416–6422.
- Jiang, J., Pang, S.Y., Ma, J., Liu, H.L., 2012. Oxidation of phenolic endocrine disrupting chemicals by potassium permanganate in synthetic and real waters. *Environ. Sci. Technol.* 46, 1774–1781.
- Jiang, J., Gao, Y., Pang, S.Y., Lu, X.T., Zhou, Y., Ma, J., Wang, Q., 2014. Understanding the role of manganese dioxide in the oxidation of phenolic compounds by aqueous permanganate. *Environ. Sci. Technol.* 49, 520–528.
- Jonsson, S., Persson, Y., Frankki, S., Bavel, B., Lundstedt, S., Haglund, P., Myskling, T., 2009. Degradation of polycyclic aromatic hydrocarbons (PAHs) in contaminated soils by Fenton's reagent: a multivariate evaluation of the importance of soil characteristics and PAH properties. *J. Hazard. Mater.* 149, 86–96.
- Kao, C.M., Huang, K.D., Wang, J.Y., Chen, T.Y., Chen, H.Y., 2008. Application of potassium permanganate as an oxidant for in situ oxidation of trichloroethylene-contaminated groundwater: a laboratory and kinetics study. *J. Hazard. Mater.* 153, 919–927.
- Kuppa, R., Moholkar, V.S., 2010. Physical features of ultrasound-enhanced heterogeneous permanganate oxidation. *Ultrason. Sonochem.* 17, 123–131.

- Lee, S.L., Ho, L.N., Ong, S.A., Wong, Y.S., Voon, C.H., Khalik, W.F., Yusoff, N.A., Nordin, N., 2016. Enhanced electricity generation and degradation of the azo dye Reactive Green 19 in a photocatalytic fuel cell using ZnO/Zn as the photoanode. *J. Clean. Prod.* 127, 579–584.
- Liang, J.Y., Ning, X.A., An, T.C., Sun, J., Zhang, Y.P., Wang, Y.J., 2016. Degradation of aromatic amines in textile-dyeing sludge by combining the ultrasound technique with potassium permanganate treatment. *J. Hazard. Mater.* 314, 1–10.
- Lin, M.Q., Ning, X.A., An, T.C., Zhang, J.H., Chen, C.M., Ke, Y.W., Wang, Y.J., Zhang, Y.P., Sun, J., Liu, J.Y., 2016. Degradation of polycyclic aromatic hydrocarbons (PAHs) in textile dyeing sludge with ultrasound and Fenton processes: effect of system parameters and synergistic effect study. *J. Hazard. Mater.* 307, 7–16.
- Lindsey, M.E., Tarr, M.A., 2000. Inhibited hydroxyl radical degradation of aromatic hydrocarbons in the presence of dissolved fulvic acid. *Water Res.* 34, 2385–2389.
- Liu, J.Y., Zhuo, Z.X., Sun, S.Y., Ning, X.A., Zhao, S.Y., Xie, W.M., Wang, Y.Y., Zheng, L., Huang, R., Li, B., 2015. Concentrations of heavy metals in six municipal sludges from Guangzhou and their potential ecological risk assessment for agricultural land use. *Pol. J. Environ. Stud.* 24, 165–174.
- Ning, X., Chen, H., Wu, J., Wang, Y., Liu, J., Lin, M., 2014a. Effects of ultrasound assisted Fenton treatment on textile dyeing sludge structure and dewaterability. *Chem. Eng. J.* 242, 102–108.
- Ning, X.A., Lin, M.Q., Shen, L.Z., Zhang, J.H., Wang, J.Y., Wang, Y.J., Yang, Z.Y., Liu, J.Y., 2014b. Levels, composition profiles and risk assessment of polycyclic aromatic hydrocarbons (PAHs) in sludge from ten textile dyeing plants. *Environ. Res.* 132, 112–118.
- Ning, X.A., Liang, J.Y., Li, R.J., Hong, Z., Wang, Y.J., Chang, K.L., Zhang, Y.P., Yang, Z.Y., 2015. Aromatic amine contents, component distributions and risk assessment in sludge from 10 textile-dyeing plants. *Chemosphere* 134, 367–373.
- Pang, S.Y., Jiang, J., Gao, Y., Zhou, Y., Hangfu, X.L., Liu, Y.Z., Ma, J., 2014. Oxidation of flame tetrabromobisphenol A by aqueous permanganate: reaction kinetics, brominated products, and pathways. *Environ. Sci. Technol.* 48, 615–623.
- Sarria, V., Parra, S., Adler, N., 2002. Recent developments in the coupling of photoassisted and aerobic biological processes for the treatment of bio-recalcitrant compound. *Catal. Today* 74, 301–315.
- Sun, B., Zhang, J., Du, J.S., Qiao, J.L., Guan, X.H., 2013. Reinvestigation of the role of humic acid in the oxidation of phenols by permanganate. *Environ. Sci. Technol.* 47, 14332–14340.
- van der Zee, F.P., Villaverde, S., 2005. Combined anaerobic-aerobic treatment of azo dyes -a short review of bioreactor studies. *Water Res.* 39, 1425–1440.
- Vogelaar, J.C.T., Keizer, A.D., Spijker, S., Lettinga, G., 2005. Bioflocculation of mesophilic and thermophilic activated sludge. *Water Res.* 39, 37–46.
- Waldemer, R.H., Tratnyek, P.G., 2006. Kinetics of contaminant degradation by permanganate. *Environ. Sci. Technol.* 40, 1055–1061.
- Zhou, T., Li, Y.Z., Wong, F.S., Lu, X.H., 2008. Enhanced degradation of 2,4-dichlorophenol by ultrasound in a new Fenton like system (Fe/EDTA) at ambient circumstance. *Ultrason. Sonochem.* 15, 782–790.